The Multivalent Adhesion Molecule SSO1327 plays a key role in *Shigella sonnei* pathogenesis

Rasha Y. Mahmoud
Daniel Henry Stones
Wenqin Li
Mohamed Emara
Ramadan A. El-domany
Depu Wang
Yili Wang
Anne Marie Krachler
Jun Yu

Summary

Shigella sonnei is a bacterial pathogen and causative agent of bacillary dysentery. It deploys a type III secretion system to inject effector proteins into host epithelial cells and macrophages, an essential step for tissue invasion and immune evasion. Although the arsenal of bacterial effectors and their cellular targets have been studied extensively, little is known about the prerequisites for deployment of type III secreted proteins during infection. Here, we describe a novel *S. sonnei* adhesin, SSO1327 which is a multivalent adhesion molecule (MAM) required for invasion of epithelial cells and macrophages and for infection *in vivo*.
The *S. sonnei* MAM mediates intimate attachment to host cells, which is required for efficient translocation of type III effectors into host cells. SSO1327 is non-redundant to IcsA; its activity is independent of type III secretion. In contrast to the up-regulation of IcsA-dependent and independent attachment and invasion by deoxycholate in *Shigella flexneri*, deoxycholate negatively regulates IcsA and MAM in *S. sonnei* resulting in reduction in attachment and invasion and virulence attenuation *in vivo*. A strain deficient for SSO1327 is avirulent *in vivo*, but still elicits a host immune response.

Introduction

Bacillary dysentery remains a significant threat to public health in the 21st century, with an estimated 160 million episodes worldwide per annum and 1.1 million deaths, of which most are children under 5 years old (Kotloff *et al*., 1999). More recent studies show that *Shigella sonnei* has indeed become the most prevalent agent in newly industrialized countries such as Korea, Republic of China, Thailand and Iran, and is more associated with dysentery in infants (Seol *et al*., 2006; Ranjbar *et al*., 2007). *S. sonnei* originated in Europe and recently disseminated globally. Fast-evolving and multidrug-resistant clones of *S. sonnei* are responsible for the current dysentery pandemic (Holt *et al*., 2012).

Shigella infection is transmitted through contaminated food or water (Chen *et al*., 2001; Leclerc *et al*., 2002). *Shigella* is highly invasive with very low infectious doses (10–100 CFU) (DuPont *et al*., 1989). Invasion occurs in the recto-colonic mucosa via M cells. Equipped with a type III secretion system (TTSS), the bacteria then invade resident macrophages as well as epithelial cells via the basolateral side. The TTSS injects the effector IpaB into macrophages, which activates caspase I (also known as interleukin I converting enzyme) and in turn triggers apoptosis to kill macrophages. Caspase I activation also results in release of activated interleukin (IL)-Iβ and IL-18, which initiates a pro-inflammatory response (Thirumalai *et al*., 1997). Upon contact with epithelial cells, the TTSS translocates a first wave of effector proteins, which cause actin rearrangements and facilitate bacterial invasion, vacuolar escape and covert intracellular replication. The intracellular bacteria then translocate via TTSS a second wave of effectors that hijack host signalling, inhibit apotosis and manipulate host innate and adaptive immunity (Schroeder and Hilbi, 2008). Via a surface protein, IcsA, the bacteria polymerize host actin that enables bacteria spread intra- and inter-cellularly (Bernardini *et al*., 1989). The lateral spread of the bacteria from cell-to-cell results in the infection and killing of neighboring epithelial cells, causing ulcers, bleeding and mucosal inflammation (Niyogi, 2005). While initial extracellular translocation of effectors is necessary to trigger invasion, intracellular growth, persistence and spread are required for virulence *in vivo*; all these events are mediated by TTSS (Schroeder and Hilbi, 2008).

Shigella originated from multiple lineages of *Escherichia coli*, and has evolved mainly through genome reduction through the action of translocation, inversion and frame shifts mediated by insertion sequences and transposons (Yang *et al*., 2005). Many genes encoding pili and fimbriae required for host attachment are inactivated in *Shigella*, and it has long been assumed that the organisms' capability to invade in a TTSS-dependent fashion has eliminated the need for adhesion (Yang *et al*., 2005). More recently, it has been demonstrated that the *Shigella flexneri* protein IcsA plays a dual role in actin-based motility and adhesion and

its role as an adhesin, which is also TTSS-dependent, is required for pathogenesis (Brotcke Zumsteg *et al*., 2014).

We are studying the molecular pathogenesis of *S. sonnei*, and found the sequenced *S. sonnei* strain Ss046 contains an intact gene encoding for a putative multivalent adhesion molecule (MAM) (SS01327), a protein of 879 amino acids with seven mammalian cell entry (MCE) domains (Fig. S1A). MAMs are widely distributed proteins in Gram-negative bacteria. The best characterized ortholog, MAM7 from the food-borne pathogen *Vibrio parahaemolyticus*, consists of an N-terminal hydrophobic region, which is required for outer membrane targeting and anchoring of the protein. This region is followed by a stretch of six to seven MCE domains which are responsible for host cell binding. MCE domains mediate binding to fibronectin and phosphatidic acid on the host cell membrane (Krachler and Orth, 2011; Krachler *et al*., 2011). MAM-mediated binding has been demonstrated to be important for pathogenicity in a numbers of pathogens, including *Yersinia pseudotuberculosis*, *Vibrio cholerae*, *V. parahaemolyticus* and enteropathogenic *E. coli* (Krachler and Orth, 2011; Krachler *et al*., 2011; Lim *et al*., 2014). Prevention of MAM-mediated binding has thus offered a new strategy in treatment of various bacterial infections (Krachler *et al*., 2012b; Hawley *et al*., 2013; Krachler and Orth, 2013).

In addition to *S. sonnei* SS01327, intact MAM *orthologs* are also present in *Shigella dysenteriae*and *Shigella boydii*. While function of the only described *Shigella* adhesin identified to date, IcsA, strictly depends on TTSS activity, MAMs are constitutively active and thus are able to establish contact between host and pathogen during the earliest stages of infection (Krachler and Orth, 2011; Krachler *et al*., 2011). This has intrigued us to investigate whether the MAM ortholog in *S. sonnei* is functional and required for virulence. Here we present evidence that MAM-mediated adherence is non-redundant with IcsA-mediated attachment. It is a prerequisite for TTSS-mediated invasion of host epithelial and phagocytic cells and necessary for *Shigella* pathogenicity *in vivo*.

Results

MAM is widely conserved across *Shigella* species

Using the sequence of the well-characterized MAM VP1611 from *V. parahaemolyticus*, we performed a search for MAM orthologs in *Shigella*. This revealed that *S. sonnei* Ss046 harbors an intact MAM ortholog, SSO1327, a putative protein of 879 amino acids sharing 35% identity and 25% similarity with *V. parahaemolyticus* VP1611. Its topology and domain organization was predicted to be highly similar to that of VP1611, containing an N-terminal

hydrophobic stretch of 41 residues and seven putative tandem MCE domains (Fig. S1A). SSO1327 is encoded on the chromosome nearby an *ipaH* pathogenicity island that carries *ipaH_3*, encoding a type III secreted effector (Fig. S1B). MAM orthologs were also identified in several other *Shigella* species, including *S. boydii* (SB01249) and *S. dysenteriae* (SDY1985), within a similar genetic context (Fig. S1B). In contrast, the *S. flexneri* MAM ortholog, SF1391, is a pseudogene, encoding for a truncated protein (Fig. S1B). To further investigate the potential biological function of the *S. sonnei* MAM SSO1327, we constructed a non-polar deletion strain in wild-type *S. sonnei* strain 20071599 (Xu *et al*., 2014), ΔSSO1327, (henceforth referred to as Δ*MAM*), (Fig. S1C–E).

Shigella MAM is localized at the bacterial outer membrane and surface exposed

Previous studies have shown that the *V. parahaemolyticus* MAM, VP1611, possesses an N-terminal hydrophobic region that allows protein targeting and anchoring to the outer membrane (Krachler and Orth, 2011; Krachler *et al*., 2011). We tested whether this was also the case for the *S. sonnei* MAM protein. As no MAM-specific antibody is available, we used the Δ*MAM* strain expressing C-terminally 6xHis-tagged MAM (Δ*MAM* + pMAM-His) to probe for protein localization. *S. sonnei* Δ*MAM* or Δ*MAM* + pMAM-His strains were grown in rich media, cells subjected to subcellular fractionation and both soluble and membrane fractions probed for the presence of MAM using α-His antibody. Fractionation was successful, as controlled for using an antibody against the outer membrane porin OmpA (Fig. 1A). MAM was exclusively detected in the membrane fraction of the MAM expressing strain, but not the deletion strain (Fig. 1A). To probe for outer membrane localization, we performed microscopy on enhanced green fluorescence protein (EGFP)-expressing bacteria treated with α-His antibody to detect MAM, followed by tetramethylrhodamine (TRITC)-labelled secondary antibody. As a control, a Δ*dsbA* strain was also transformed to express DsbA-His, which is a periplasmic protein required for *Shigella* virulence (Yu *et al*., 2000). While MAM-His was detected both in Triton-treated and untreated bacteria (Fig. 1Bii, and 1Cii, respectively), DsbA-His was only detected in Triton-treated, but not untreated cells (Fig. 1Eii and 1Dii, respectively). Triton-X100 is able to permeabilize the outer membrane, which renders the periplasmic DsbA-His accessible to the antibody. As MAM-His was detected in the absence of permeabilization, these data demonstrate that, like its orthologs, *S. sonnei* MAM localizes to the bacterial outer membrane, with the C-terminus oriented toward the extracellular side.

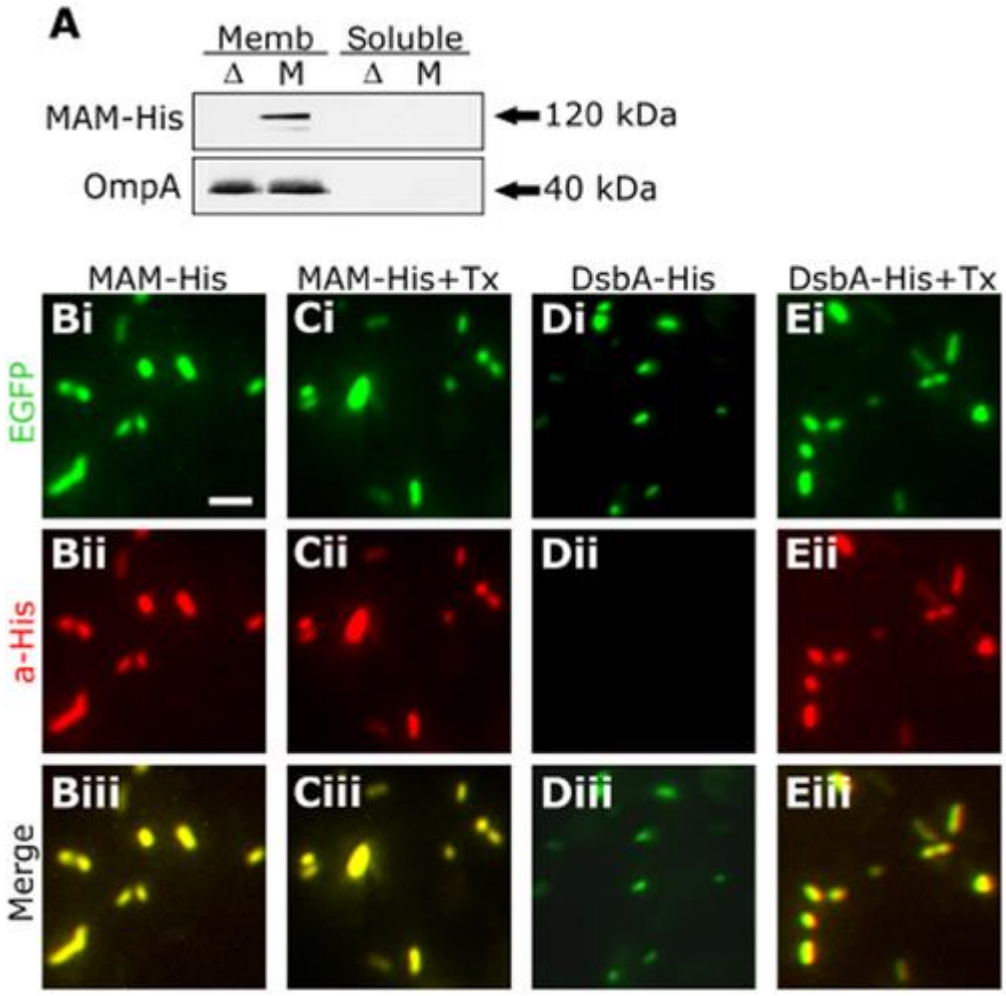

Figure 1

The *Shigella sonnei* MAM is localized at the bacterial outer membrane.

A. *S. sonnei* Δ*MAM* (Δ) and complementation strain (Δ*MAM* + pMAM-His, M) were grown to mid-log phase and soluble and membrane fractions separated by SDS-PAGE. MAM and OmpA (OM protein, fractionation control) were detected by Western blotting using antibodies against His-tagged MAM and OmpA, respectively.

B, C, D, E. Strains Δ*MAM*/pMAM-His and *ΔdsbA*/pDsbA-His expressing EGFP were treated with or without Triton X-100, and anti-His antibodies, followed by TRITC-labelled secondary antibodies. EGFP-*Shigella* (green), MAM-His and DsbA-His (red), and merged channels are shown. Scale bar = 5 μm.

MAM and IcsA are two non-redundant *Shigella* adhesins required for attachment to and invasion of host cells

Shigella attaches to and invades both epithelial cells and macrophages in a TTSS-dependent manner. Although the contribution of TTSS structural components and effector proteins to these processes has been carefully evaluated in the past, until recently, nothing was known about factors required to initiate the intimate contact between bacteria and host cells that is necessary to trigger initial TTSS-dependent translocation of effectors that facilitate invasion. Recently, IcsA has been described to be involved in bacteria–host association in *S. flexneri*. Thus, we tested the contribution of MAM and IcsA to *S. sonnei* attachment and invasion, both individually and in combination.

First, we tested both *S. sonnei* wild-type and deletion strains for adherence to HeLa epithelial cells, which are a widely used model for assessing bacterial adhesion and invasion. Adherence levels in the Δ*MAM* and the Δ*icsA* deletion strains dropped similarly to ~25–20% compared with wild-type levels (statistically significant, $P < 0.05$). The wild-type strain's attachment capacity could be restored by complementation of the deletion strains with MAM or IcsA, respectively, expressed *in trans* (Fig. 2A). A Δ*MAM*/Δ*icsA* double mutant showed further reduction in adherence to less than 20% compared with the wild type, indicating a synergistic effect between MAM and IcsA. This double mutation could be completely complemented to restore wild-type levels of attachment, by expressing both MAM and IcsA from a single plasmid, pMI, *in trans*. We further tested the growth kinetics of wild-type and all mutant strains (Fig. S7), and all strains grown equally well in L-broth, ruling out growth defects as a reason for the different attachment and invasion phenotypes we observed. Thus, we conclude that IcsA and MAM contribute equally to adherence and that there is synergy between the two adhesins. As the double mutant still retained low levels of adherence, other, as yet unidentified factors may mediate adherence in the Δ*MAM*/Δ*icsA*background.

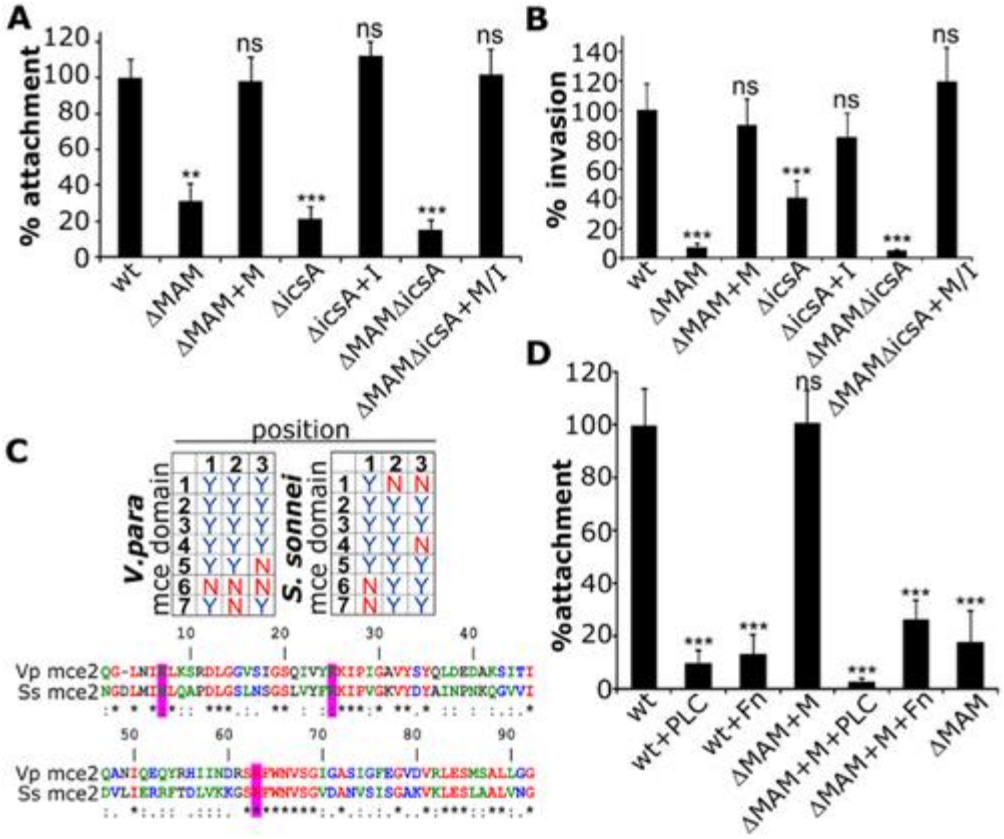

Figure 2

Functional characterization of *Shigella sonnei* MAM and IcsA in host cellular adhesion and invasion.

A. Attachment of *S. sonnei* strains to HeLa cells following a 15 min infection at an MOI of 30 was determined by Triton X-100 lysis and plating.

B. Invasion of HeLa cells was determined by gentamycin protection experiments following 2 h of infection at an MOI of 10.

C. Conservation (Y) or absence (N) of basic residues (H/K/R) at key positions required for high affinity phosphatidic acid binding within MCE domains 1–7 of *Vibrio parahaemolyticus* and *S. sonnei* MAMs. Sequence based alignment is shown for MCE2 domains, with key conserved PA-binding residues highlighted in pink.

D. Attachment of wild-type and complemented MAM deletion strain to HeLa cells, which were left untreated or treated with phospholipase C (+ PLC) or preincubated with fibronectin (+Fn). All results are means ± standard deviation ($n = 3$). Significance of results compared with those for the wild-type strain was determined using a *t*-test: (*) $P = 0.0163$, (**) $P = 0.0021$, (***) $P < 0.0001$.

Shigella is well-known for its ability to invade host cells; the significance of attachment in pathogenesis has only been investigated regarding IcsA's role, which is otherwise known to be required for actin-based cellular motility. Therefore, we investigated whether deletion of the *S. sonnei* MAM led to reduced invasiveness, using 2 h gentamycin protection assays. Deletion of *icsA* reduced invasion to 40% of the wild-type levels and deletion of *MAM* caused more profound reduction to less than 10% of the wild-type levels (Fig. 2B). Expression of MAM or IcsA *in trans*, respectively, restored invasiveness in full to these two mutants. Removal of *MAM* and *icsA* together caused slightly more reduction than removal of *MAM*alone, indicating that MAM plays a more important role than IcsA in invasion (Fig. 2B). Expressing both MAM and IcsA from pMI *in trans* fully complemented the double mutant for invasion (Fig. 2B).

In *V. parahaemolyticus*, attachment of the MAM VP1611 to host cells is dependent on two host surface receptors; direct, high-affinity binding of MCE domains to phosphatidic acid membrane phospholipids via key conserved basic residues in each domain is necessary for adhesion, while fibronectin acts as a co-receptor and accelerates surface engagement (Krachler and Orth, 2011). A comparative analysis of key basic residues reportedly involved in phosphatidic acid binding by VP1611, and the *Shigella* MAM SSO1327 revealed a high level of conservation of basic residues in key lipid binding positions (Fig. 2C). Thus, we tested the requirement of *S. sonnei* MAM for phosphatidic acid and fibronectin in host cell adherence. Treatment of epithelial cells with phospholipase C (PLC) depletes phosphatidic acid from the membrane (Lim *et al*., 2014). Following PLC treatment, bacterial adhesion to host cells was decreased to ~ 10% of wild-type levels, and levels comparable with those observed for *ΔMAM* attachment (Fig. 2D). The requirement for fibronectin was evaluated using a competition assay. Pre-incubation of bacteria with fibronectin from human plasma significantly decreased attachment to epithelial cells, albeit to a lower extent than phosphatidic acid depletion. We conclude that *S. sonnei* MAM has similar binding specificity and host receptor requirements as the *V. parahaemolyticus* MAM VP1611 and engages both phosphatidic acids and fibronectin at the host cell surface. We also noted that blocking or eliminating host cell receptors was more efficient in inhibiting attachment than deleting MAM (Fig. 2A vs. 2D). This may suggest that other, yet unidentified, adhesins also use PA and fibronectin for attachment.

MAM is not involved in production or secretion of type III effectors, but enables efficient substrate translocation into host cells

Shigella invasion is dependent on a functional TTSS, and the secreted components IpaB and IpaC are known to form a translocon pore complex in the target cell membrane and facilitate the injection of effector proteins into the host cell cytoplasm to initiate invasion (Menard *et al*., 1994; Veenendaal *et al*., 2007). Therefore, we investigated whether removal of MAM reduced secretion of IpaB and IpaC, by use of Congo red as environmental cues for secretion *in vitro* as described previously (Bahrani *et al*., 1997). Similar levels of IpaB and IpaC were detected in the total cell lysates and supernatants of wild-type, Δ*MAM* mutant as well as the complemented *ΔMAM* strain (Fig. 3A). Thus, removal of MAM neither affects TTSS protein production nor secretion.

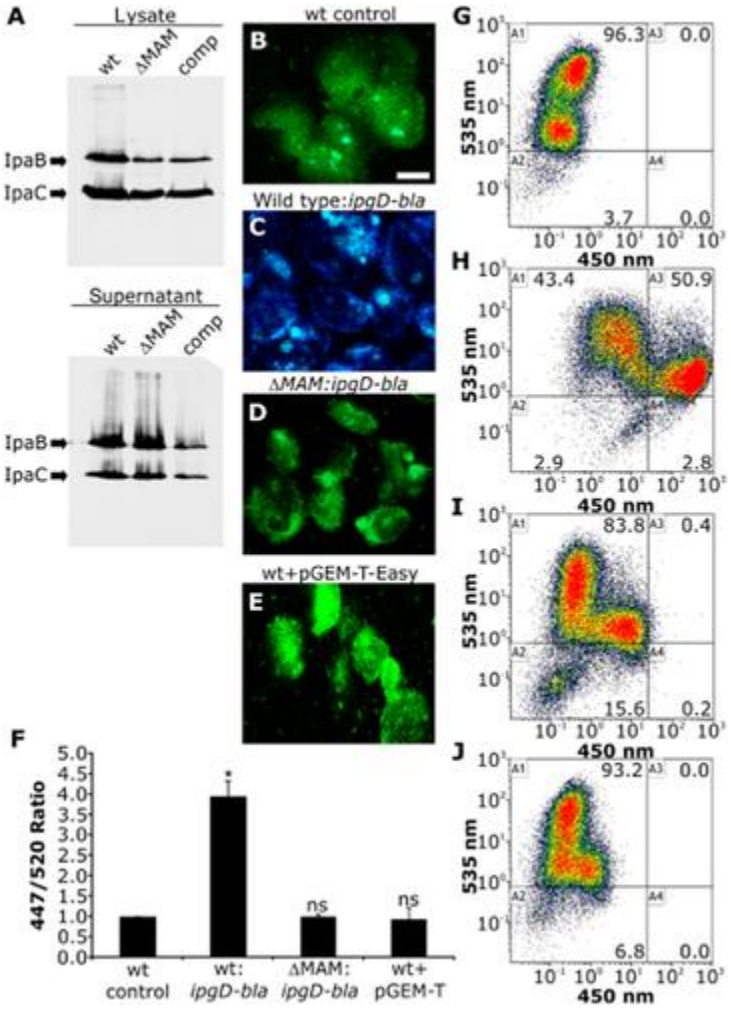

Figure 3

Analysis of *Shigella sonnei* MAM role in production, secretion and translocation of type III secretion system substrates.

(A) S. sonnei wild type, Δ*MAM* or Δ*MAM*/pMAM-His strains were grown to mid-log phase, type III secretion was induced with Congo red and cell lysates and culture supernatants analyzed for the presence of type III system secreted effectors by SDS-PAGE and Western blotting with antibodies against IpaB and IpaC. HEK293 cells were either mock infected (B and G), or infected with *S. sonnei* wild-type (C, H) or Δ*MAM* (D, I) strains carrying chromosomal *ipgD-bla* fusions or wild type carrying pGEM-T-Easy (E, J). Substrate translocation was analyzed by FRET imaging (B–E). Scale bar, 10 μm. Results of ratiometric image analysis are means ± standard deviation (F: $n = 3$). Significance of results compared with those for the control (mock infection) was determined using a *t*-test and asterisks indicate *P*-values < 0.001. ns: not significant. Substrate translocation was also analyzed by flow cytometry (G–J). Marked increase of donor (450 nm) and decrease of acceptor fluorescence (535 nm) was observed in cells infected by wild-type strain compared with cells infected by Δ*MAM* strain or cells infected by wild-type strain carrying pGEM-T-Easy (H vs. I; H vs. J).

Translocation of TTSS effector proteins into the host cell cytoplasm requires prolonged and intimate contact between bacteria and host cells. Thus, we investigated if the absence of MAM negatively affects the initial translocation of type III secreted effector proteins from adherent bacteria into host cells. HEK293 cells were loaded with the β-lactamase (Bla) cleavable substrate CCF4-AM and infected with *Shigella* wild-type or Δ*MAM* reporter strains carrying a chromosomal fusion of Bla to the TTSS effector IpgD (*ipgD-bla*), which is implicated in actin rearrangements, which facilitate bacterial invasion of non-phagocytic cells upon host cell contact (Niebuhr *et al*., 2000). We included a negative control, wild-type strain carrying p-GEM-T-Easy, which expresses β-lactamase, but will not be able to translocate it into host cells. Substrate translocation was analyzed by ratiometric analysis of imaged cells and by flow cytometry. While substrate loaded mock-infected cells fluoresce green (Fig. 3B and G), wild-type infection lead to translocation of IpgD-Bla into the host cell cytoplasm, which was marked by substrate cleavage and a shift toward blue fluorescence within 50 min post-infection (Fig. 3C and H). Little translocation and thus, little shift in fluorescence, was observed during infection with the Δ*MAM* reporter strain and the wild-type strain carrying pGEM-T-Easy (Fig. 3D and I, and E and J, respectively), although all strains displayed similar levels of β-lactamase activity (Fig. S2). Taken together, these experiments suggest that although the presence of MAM is not required for TTSS effector secretion, it is necessary to achieve intimate contact between bacteria and host cells required for effector translocation.

MAM is required for *S. sonnei* pathogenesis and interaction with phagocytes *in vivo*

Larvae of the wax moth *Galleria mellonella* are an abundantly used *in vivo* infection model, including those with enteric pathogens such as enteropathogenic *E. coli* (EPEC) and *Salmonella* (Leuko and Raivio, 2012; Viegas *et al*., 2013). It is particularly suited to study interactions between pathogens and phagocytic cells in a living organism (Harding *et al*., 2012). To test the function of *S. sonnei* MAM during pathogenesis, larvae were infected with doses of either 10^5 or 10^6 CFU of *S. sonnei* wild-type, Δ*MAM* or complemented Δ*MAM* + pMAM strains by injection into the front, right proleg. Control animals were injected with the same volume of sterile PBS. Larvae infected with 10^6 CFU of *S. sonnei* wild-type strain all succumbed to infection within one day (Fig. S4). Larvae infected with 10^5 CFU of wild-type *S. sonnei* showed a pronounced phenotype with rapid melanization indicative of an immune response and loss of mobility, and succumbed to infection between days 1 and 5 following infection (Fig. 4A and E). In contrast, larvae infected with 10^5 CFU Δ*MAM* showed lower mortality, with 70% of animals alive on day 5 (Fig. 4B and E). Expression of MAM *in trans*restored mortality rates to wild-type levels (Fig. 4C and E), while all control animals lived beyond day 5 (Fig. 4D and E).

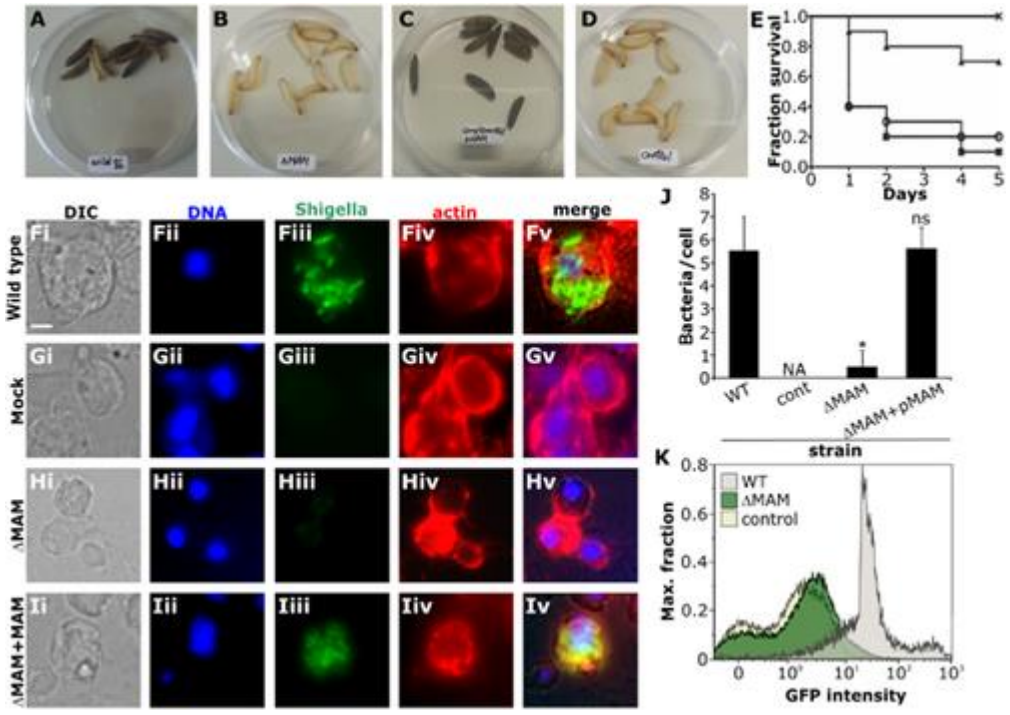

Figure 4

MAM is required for *Shigella sonnei* pathogenesis and interaction with phagocytes *in vivo.*

Two- to 3-day-old *G. mellonella* larvae were injected with a dose of 10^5 CFU of *S. sonnei* wild type (A), Δ*MAM* (B), Δ*MAM* + pMAM-His (C) or an equivalent volume of sterile buffer (D) and imaged on day 2. Larval mortality of animals injected with buffer (control, crosses), or 10^5 CFU of wild type (black square), Δ*MAM* (black triangles) or Δ*MAM* + pMAM-His (empty circles) was followed over five days and data shown as Kaplan–Meier survival curves (E). Hemocytes were isolated from the hemolymph of larvae infected with *S. sonnei* wild type (F), mock infected (G), or infected with Δ*MAM* (H) or Δ*MAM* + pMAM-His (I) at 10^5 CFU for 4 h. Samples were visualized by microscopy and DIC (grey), Hoechst (blue), GFP *Shigella* (green), F-actin (red) and merged images are shown. Scale bar, 5 μm. Bacteria per cell were quantified by image analysis (J) and at least 100 hemocytes were analyzed per experimental condition. NA: not analyzed. Alternatively, hemocytes (infected with wild-type *S. sonnei*, grey or Δ*MAM*, green) or mock infected (yellow trace) were analyzed for GFP fluorescence by flow cytometry (K). All results are means ± standard deviation ($n = 3$). Significance of results compared with those for the wild-type strain was determined using a *t*-test and asterisks indicate *P*-values < 0.0001. ns, not significant. Also see Fig. S3.

Shigella sonnei virulence in the *G. mellonella* larval model was strongly correlated with the bacteria's ability to invade phagocytes. To understand the underlying mechanisms of larval killing by *Shigella*, hemolymph was collected from larvae infected with EGFP expressing *S. sonnei* strains, and used to isolate infected phagocytes. Bacterial burden inside phagocytes was evaluated both by flow cytometry and fluorescence microscopy. More than 75% of hemocytes isolated from larvae infected with wild-type *S. sonnei* contained a high bacterial burden of approximately five bacteria per cell on average (Fig. 4F). In contrast, phagocytes isolated from Δ*MAM* infected larvae essentially lacked intracellular bacteria (average burden of less than one bacterium per cell) and were practically indistinguishable from uninfected phagocytes both by flow cytometric and microscopic analysis (Fig. 4G, H, K). Expression of MAM *in trans* restored wild-type levels of bacterial burden and eventual lysis (Fig. 4I and J). *G. mellonella* hemocytes possess similar properties than macrophages from vertebrates (Harding *et al*., 2012). *Shigella* infection typically causes macrophage apoptosis via the action of IpaB (Thirumalai *et al*., 1997). Therefore, we investigated whether *S. sonnei* causes apoptosis to *G. mellonella* hemocytes. Apoptotic macrophages typically produce fragmented chromatin, which can be detected by agarose gel electrophoresis (Zychlinsky *et al*., 1992). We isolated and analyzed total DNA from *Shigella* infected and uninfected moth larvae. Chromatin fragmentation was apparent in DNA samples isolated from wild type infected, but not Δ*MAM* or mock-infected larvae (Fig. S3). Thus, *S. sonnei* invaded and caused apoptosis to larvae hemocytes, mirroring the mechanism of killing observed in vertebrates.

MAM-coupled polymer beads mimic bacterial attachment and are protective against *Shigella* infection

Previous studies showed MAM chemically coupled to polymer beads can mimic bacterial adhesion and competitively exclude pathogens from the host cell surface, thus attenuating infection (Krachler *et al*., 2012a). We investigated whether MAM-coupled beads would be protective against *S. sonnei* infection *in vivo*, using the *G. mellonella* larval model. MAM-displaying beads were co-injected with doses of either 10^5 or 10^6 CFU of wild-type *S. sonnei*and larvae survival monitored over time. MAM beads administered at the same time as *S. sonnei* inhibited infection (Fig. 5B) while control beads had no protective effect (Fig. 5C). Dosing experiments revealed that MAM beads inhibited infection with a dose of 10^5 CFU to concentrations of 6 µM. At 10^6 CFU, a dose that killed all unprotected larvae within one day, co-injection with MAM beads attenuated infection in a concentration-dependent manner (Fig. S4). An inhibitor concentration of 25 µM protected 90% of larvae beyond day 5 post-infection (Fig. S4). The lowest inhibitor concentration used (6 µM) protected 50% of larvae beyond day 5. The protective effect of beads was due to their ability to block host cell invasion *in vitro* and *in vivo*, by competitively excluding *Shigella* from binding to the host surface receptors (Fig. 5E–I). The beads had no visible effect on phagocyte morphology (Fig. 5G) and did not interfere with TTSS effector production or secretion (Fig. S5).

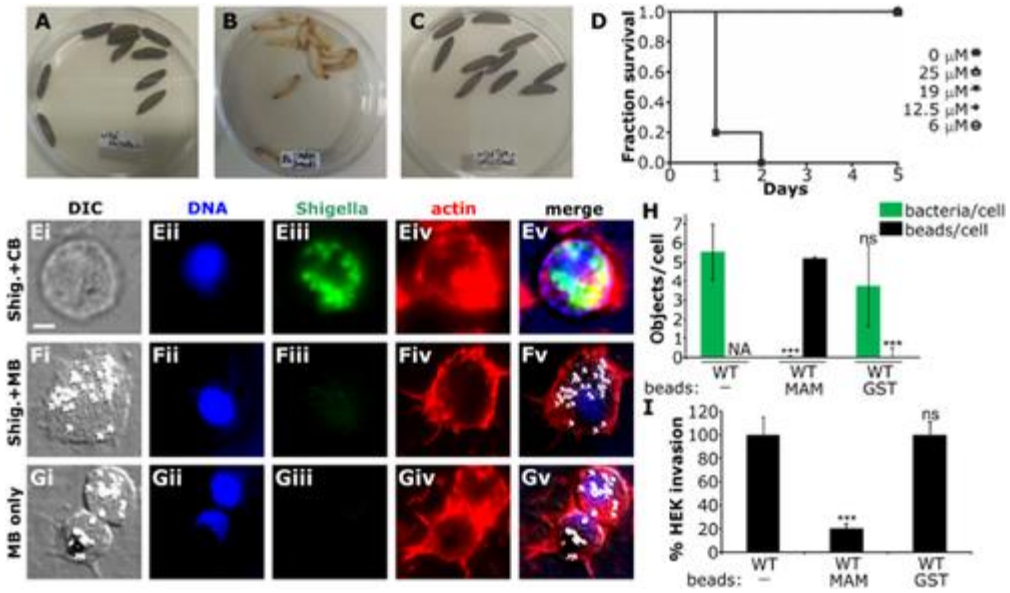

Figure 5

A MAM mimetic adhesion inhibitor can efficiently protect against *Shigella sonnei* invasion and pathogenesis.

Galleria mellonella larvae were injected with 10^5 CFU *S. sonnei* wild type (A), a mixture containing 10^5 CFU *S. sonnei* and 25 μM MAM beads (B) or a mixture containing 10^5 CFU *S. sonnei* and 25 μM GST (control) beads (C) and imaged on day 2. Mortality rates over 5 days of larvae injected with 10^5 CFU wild type and either buffer (black squares), or MAM beads at a final concentration of 25 (empty triangles), 19 (black triangles), 12.5 (dotted line) or 6 μm (empty circles) were analyzed using Kaplan–Meier survival curves (D). Hemocytes were isolated from larvae injected with a mixture containing 10^5 CFU *S. sonnei* and 25 μM GST (control) beads (E), a mixture containing 10^5 CFU *S. sonnei* and 25 μM MAM beads (F) or 25 μM MAM beads but no bacteria (G). Samples were visualized by microscopy and DIC (grey), Hoechst (blue), GFP *Shigella* (green), F-actin (red) and merged images are shown. Scale bar, 5 μm. Bacteria per cell (green bars) and beads per cell (black bars) were quantified by image analysis, and at least 100 hemocytes were analyzed per experimental condition (H). NA: not analyzed. The effect of MAM beads or control (GST) beads on bacterial invasion of HEK293 cells was determined using gentamycin protection assays and compared with invasion of untreated (−) cells (I). Results are means ± standard deviation ($n = 3$). Significance of results was determined using a *t*-test and asterisks indicate *P*-values < 0.0001. ns: not significant. Also see Figs–S3 and S4.

MAM is required for *S. sonnei* induced keratoconjunctivitis and immunization with MAM-deficient *Shigella* induces limited protective immunity

Although the above data demonstrated the usefulness of *G. mellonella* larvae as a model for *Shigella* infection, we also exploited the more established guinea pig keratoconjunctivitis model to further characterize the MAM mutant. *Shigella* strains, wild-type and *ΔMAM* mutant, as well as PBS (mock infection) were administered into the eyes (three animals in each group) and animals monitored for development of keratoconjunctivitis. *S. sonnei* wild-type strain caused all three animals fully developed keratoconjunctivitis by day 3 (Fig. 6A and B), whereas the Δ*MAM* mutant did not cause any sign of the disease up to 14 days post-infection in any of the animals (Fig. 6C and D). At this point, we tested if the attenuated Δ*MAM* mutant could be used as a vaccination strain. Therefore, we administered the same guinea pigs with Δ*MAM* mutant at days 14 and 28 to boost immunization and challenged the animals with wild-type strain at day 33. Surprisingly, none of the animals showed any sign of conjunctivitis until day 36. After this, the symptoms progressed slowly for the worse and full keratoconjunctivitis was developed by day 41. To compare the immune responses elicited by the wild type and the Δ*MAM* mutant, we collected guinea pig spleens for detecting antibody secreting cells (ASC) specific

to *S. sonnei* lipopolysaccharide. The Δ*MAM* mutant elicited similar levels of ASC than the wild-type strain following ocular administration to guinea pigs (Fig. 6E).

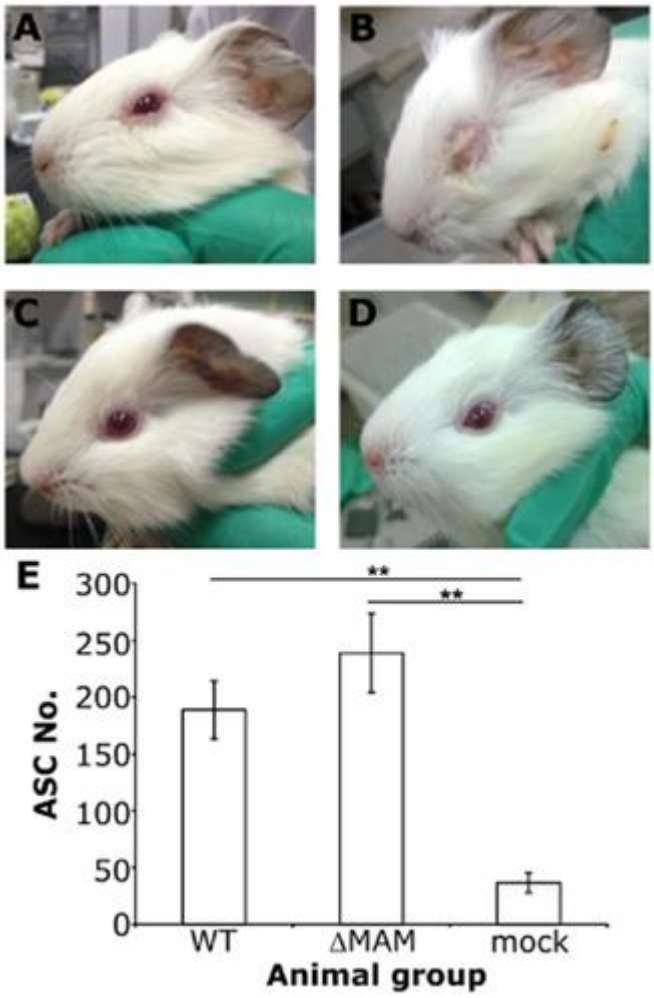

Figure 6

Role of MAM in a keratoconjunctivitis model of *Shigella* infection and immunity.

(A–D) Sereny test. Guinea pigs ($n = 3$) were infected with 5×10^8 CFU of bacteria per eye. All animals infected with wild-type *S. sonnei* developed full keratoconjunctivitis in 3 days. Animals infected with Δ*MAM* strain did not show any sign of conjunctivitis up to 14 days. Animals before (A) and after (B) infection with wild type and before (C) and after (D) infection with Δ*MAM* deletion strain for five days are shown. E. ELISPOT data. Animals in group 1 (gp/Wt) were immunized with Δ*MAM* three times and challenged with wild-type *S. sonnei*; animals in group 2 (gp/delMAM) immunized with Δ*MAM* strain four times; animals in group 3 were mock infected with PBS four times. Both group 1 and group 2 animals produced significantly higher antibody secreting cells (ASC) specific to *S. sonnei* LPS in spleen lymphcytes compared with group 3 mock-infected animals (**

indicate $P < 0.001$). The difference between group 1 and group 2 animals are not statistically significant ($P = 0.05$).

Deoxycholate (DOC) negatively regulates *S. sonnei* pathogenicity *in vitro* and *in vivo*

Brotcke Zumsteg *et al*. (2014) have recently described positive regulation of *S. flexneri* by DOC in adherence and invasion to host cells, which are partially dependent on IcsA. We therefore investigated whether this is also the case for *S. sonnei*. First, wild-type, Δ*MAM* and Δ*icsA*strains were tested for their adherence to HeLa cells with or without DOC treatment (Fig. 7A). Adherence was decreased by DOC in wild-type and all single-deletion strains. DOC equally decreased invasion of HeLa cells by wild-type and all mutant strains (Fig. 7B). Next, transcription levels of *MAM* and *icsA* in the presence and absence of DOC treatment were compared using quantitative polymerase chain reaction (qPCR) analysis. DOC significantly reduced transcription of both *MAM* and *icsA* (Fig. 7C), which was consistent with the attachment and invasion data.

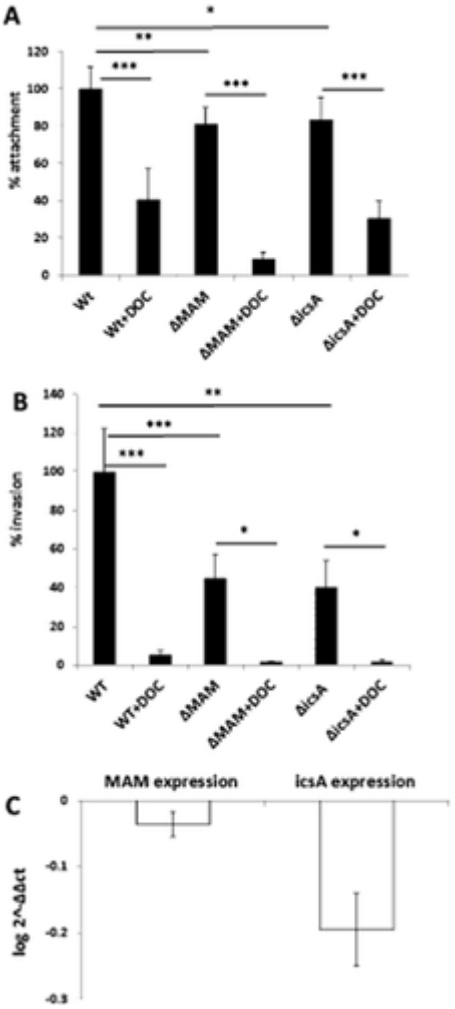

Figure 7

Deoxycholate negatively regulates *MAM* and *icsA* in *Shigella sonnei*.

Attachment of *S. sonnei* strains either grown in LB or LB containing deoxycholate (+ DOC) to HeLa cells following a 15 min infection at an MOI of 30 was determined by Triton X-100 lysis and plating (A). Invasion of HeLa cells was determined by gentamycin protection experiments following 2 h of infection at an MOI of 10, either following growth in LB or LB containing DOC (+ DOC), (B). All results in A, B are means ± standard deviation ($n = 3$). Significance of results compared with those for the wild-type strain was determined using a *t*-test: $*P < 0.05$, $**P < 0.01$, $***P < 0.0001$. (C) qPCR analysis of *MAM* and *icsA* transcription upon deoxycholate treatment. Data present mean values from triplicate cultures ($n = 3$) for each strain.

Finally, the effect of DOC on *S. sonnei* virulence *in vivo* was investigated in both the guinea pig keratoconjunctivitis and moth larvae models. DOC treatment significantly delayed the onset of conjunctivitis and reduced disease severity in guinea pigs (Fig. S6A) and also significantly protected moth larvae from killing by wild-type as well as all mutant strains of *S. sonnei* (Fig. S6B).

Discussion

MAM-mediated attachment is required for translocation of TTSS substrates into host cells

In this study, we have demonstrated that SSO1327 encodes a functional MAM, which is expressed on the bacterial surface (Fig. 1) and involved in bacterial attachment to host cells, a key step during molecular pathogenesis (Fig. 2). Furthermore, we show that this initial step is essential for the translocation of a first wave of effectors, including IpgD, into host cells, which facilitates subsequent invasion. It is known that *Shigella* bacteria can be internalized 15 min after contacting HeLa cell monolayers (Mounier *et al*., 1997). Thus, although the initial attachment via adhesins and TTSS-mediated invasion of non-phagocytic cells are two distinctive events they occur rapidly in a continuing fashion. The graphs presented in Fig. 2A and D for attachment are likely to be a total sum of large numbers of extracellular and small numbers of intracellular *S. sonnei*. For scope of this study, it was unnecessary to exhaustively analyze the contribution of each of these two populations of bacteria. Most importantly, we have demonstrated that the deletion of MAM causes a decrease in initial cell-associated bacteria, which has a knock-on effect on invasion as shown in Fig. 2B. We further show that

decreased adherence leads to inefficient translocation of early TTSS effectors from extracellular bacteria into the host cells cytoplasm, which implies strongly that both the decrease in attachment as well as the impairment of effector translocation play a role in the observed invasion deficiency. Like its ortholog from the sea-foodborne pathogen *V. parahaemolyticus*, *S. sonnei* MAM specifically binds to fibronectin and phosphatidic acids (Fig. 2D). Most strikingly, failure to adhere to the host cell surface, either by deletion of the *MAM*gene or by competitive inhibition of MAM-mediated binding using MAM-based, synthetic beads, leads to a significant reduction of cell invasion and host protection in a moth larvae infection model (Figs 2 and 4). Deletion of *MAM* does not cause a secretion defect, as in the absence of MAM both IpaB and IpaC were still produced and secreted in response to the environmental cue, Congo red (Fig. 3A). This suggests that MAM does not directly impact on the function of TTSS. Conversely, TTSS function is not needed to achieve MAM-mediated binding, as was previously shown in *V. parahaemolyticus* (Krachler and Orth, 2011; Krachler *et al*., 2011). Thus, we conclude that in contrast to IcsA, MAM and TTSS are mutually independent. However, bacteria fail to inject effector proteins into host cells, when MAM-mediated attachment is abrogated by MAM gene deletion (Fig. 3). This finding suggests the following as a likely scenario: MAM-mediated intimate attachment brings the bacteria within close proximity of the cell membrane, allowing TTSS to engage with the cells' membrane for activation. It is known that *Shigell*a TTSS activation requires the formation of a translocon on the host cell membrane (Veenendaal *et al*., 2007). This event can only occur when *Shigella* is within close proximity of the host cell surface. MAM is relatively small compared with other known adhesion molecules, such as flagella and pili (Jaglic *et al*., 2014). Therefore, intimate adherence by MAM may be required to bring *Shigella* within close enough proximity to the host cell surface to allow TTSS translocon formation on the host cell membrane. It is known that *Shigella* TTSS is also responsible for bacterial escape from the phagocytic vacuoles into the cell cytosol and cell-to-cell spread (High *et al*., 1992; Page *et al*., 1999). Whether *Shigella*MAM plays a part in these events as well as in translocation of late effectors during intracellular growth requires further investigations.

Recently, another surface protein, IcsA, has been described to mediate attachment of *S. flexneri* to the host cell surface, in addition to its role in actin based motility inside the host cells (Brotcke Zumsteg *et al*., 2014). In *S. sonnei*, IcsA's role is not redundant with MAM so both adhesins may be required during different stages of the infection process. In *S. flexneri*, IcsA-mediated attachment depends on TTSS activity and, similar to TTSS function, is activated by bile salts, which leads to IcsA adopting an altered, protease resistant and attachment competent conformation (Brotcke Zumsteg *et al*., 2014). In *S. sonnei*, we also found IcsA to be necessary for adhesion and invasion (Fig. 2), but DOC caused a reduction in attachment and invasion by the wild-type as well as the mutant strains (Fig. 7A and B). qPCR

analysis confirmed that DOC caused significant reduction of MAM and IcsA transcription (Fig. 7C). The attenuation of virulence by DOC was further confirmed by Sereny test and in our newly established moth larvae model (Fig. S6A and S6B). The differential effect of DOC to *S. flexneri* and *S. sonnei* may explain why *S. sonnei* is less virulent and requires a much higher infectious dose to cause disease (DuPont *et al*., 1989).

As noted earlier, the MAM gene in *S. flexneri* strain 301 (Sf1391) is a pseudogene because of an in frame stop codon (Yang *et al*., 2005). Thus, *S. flexneri* may have evolved different regulatory mechanisms to coordinate IcsA-mediated attachment and TTSS. According to available genome sequences, a number of *S. flexneri* strains have the same in-frame stop codon; they are Shi06HN006, 2003036, 2002017, 8401, and 2457T. We have also confirmed by PCR-sequencing that strain M90T, used by (Brotcke Zumsteg *et al*., 2014) has the same mutation (data not shown). On the other hand, three *S. flexneri* genomes appear to have intact MAMs; AFGY01000021.1, AKMV010000023.1, and AKMY01000025.1. The significance of IcsA attachment in these strains with intact MAM genes remains to be investigated. Investigations to compare *S. flexneri* strains with and without intact MAM genes would help us gain a more detailed understanding of the regulation of attachment and cell invasion by DOC.

Brotcke Zumsteg *et al*. (2014) also observed IcsA-independent attachment. Although the molecular basis for IcsA-independent attachment is unknown, MAM is unlikely to be involved as it is heavily truncated in this strain. Many genes involved in adherence are all lost in representatives of four groups of *Shigella* strains, due to genome reduction, including fimbriae, pili and flagella (Yang *et al*., 2005). At the time of genome annotation MAM was not recognized. But, an intact orthologue of YadA from *Yersinia pestis* was noted in the genome of *S. sonnei* strain Ss046. The YadA orthologs in the other three classes of *Shigella* all possess significant truncations at the C-termini (Yang *et al*., 2005). YadA mediates effective attachment of *Y. pestis* to host cells and improves the delivery of the TTSS effector protein YopE (Rosqvist *et al*., 1990). Whether the truncated YadA is functional and responsible for the observed IcsA-independent attachment in *S. flexneri* remains to be investigated. But, *S. sonnei*YadA is the prime suspect responsible for the residual attachment of the *ΔMAMΔicsA* double mutant observed (Fig. 2A). YadA mediates effective attachment of *Y. pestis* to host cells through binding to fibronectin and β1 integrin (Eitel and Dersch, 2002) and improves the delivery of the TTSS effector protein YopE (Rosqvist *et al*., 1990). Thus, the significance of the YadA ortholog in *S. sonnei* certainly deserves further investigation.

G. mellonella larvae infection model

Non-human primate (NHP) rhesus monkeys (*Macaca mulatta*) are natural hosts of *Shigella*, with an infection phenotype that mimics human dysentery (Islam *et al*., 2014). This non-human primate model is however very costly. Therefore, other animal models such as the murine lung and rabbit ligated ileal loop models have been developed for defining some of the immune and inflammatory components of the disease (Philpott *et al*., 2000). Recently, the great moth, *G. mellonella*, has gained popularity as a model for assessing virulence and a number of pathogens have been studied using this model, including enteropathogenic *E. coli* (EPEC), *Salmonella typhimurium* and *Listeria monocytogenes* (Leuko and Raivio, 2012; Harding *et al*., 2013; Viegas *et al*., 2013). To our knowledge, this study is the first to report the use of this model for assessing virulence of *Shigella*. Wild-type *S. sonnei* kills *G. mellonella* larvae in a dose-dependent manner, and mutations in MAM and other virulence genes greatly increased larvae survival (e.g., Fig. 4). More importantly, our results have revealed that larvae killing by wild-type *S. sonnei* is in part due to bacterial invasion of hemocytes, which eventually undergo apoptosis (Fig. 4 and Fig. S3). Deletion of the MAM gene or application of MAM-based synthetic beads leads to reduced invasion of hemocytes and apoptosis (Fig. 5). Hemocytes possess characteristics of vertebrate macrophages (Harding *et al*., 2012). Induction of apoptosis in hemocytes is consistent with induction of apoptosis in human macrophages, due to activation of caspase I by secreted IpaB (Chen *et al*., 1996). Homologs to human caspases have been identified in *G. mellonella* and are involved in tissue remodelling during metamorphosis (Khoa *et al*., 2012). However, their characterization has been limited by the absence of a whole genome sequence and little is known about their role during infection.

The results we obtained in the *Galleria* larvae model were consistent with those obtained using the well-established guinea pig keratoconjunctivitis model. Wild-type *S. sonnei* induced full kertatoconjunctivitis within 3 days, whereas the MAM mutant failed to produce visible signs of the disease (Fig. 6). Our unpublished data show that several other mutations in well-defined virulence genes, including *mxiD, ipaB* and *dsbA*, also resulted in decreased mortality in the *Galleria* larvae, consistent with these strains' inability to cause conjunctivitis in the Sereny test. Taken together, these data indicate *Galleria* larvae are a suitable initial model for studying *Shigella* virulence and encourage its use for future studies. Our study along with others, also calls strongly for sequencing the genome of *G. mellonella*.

Potential of MAM deletion strains as a new strategy for vaccine development

Deletion of *icsA* attenuates *Shigella* virulence in the Sereny test (Brotcke Zumsteg *et al*., 2014). This has been the basis of development of live attenuated vaccines,

some of which are currently undergoing clinical trials (Rahman *et al*., 2011; Camacho *et al*., 2013). Although some of these candidates have shown promising results, their efficacy especially in endemic regions has proven insufficient (WHO, 2006). Our results show that a *S. sonnei* MAM deletion strain leads to attenuation of virulence in the guinea pig eye infection, but still elicited strong immune responses (Fig. 6). Thus, deletion of MAM may be an alternative approach in engineering future live attenuated vaccines for *S. sonnei*.

The potential of using MAM as a target for therapy or vaccination

The use of MAM-based synthetic beads as an adhesion inhibitor has shown potential in the prevention of a number of bacterial infections, in particular in treating *Pseudomonas* infection of burns and wounds (Krachler *et al*., 2012a,b). Our results show clearly that applying MAM-coupled polymer beads can reduce *S. sonnei* invasion of cultured host cells and protect *Galleria* larvae from *S. sonnei* infection (Fig. 5). These data call for further investigations into the potential of MAM-based adhesion inhibitors for therapy and vaccination. One uncertainty is whether a sufficient amount of beads could reach the intestinal tract following oral dosing. Dosing is easily controlled following topical application of beads to skin. However, it is hard to estimate how much inhibitor would be required via oral administration to ensure a sufficiently high concentration at the site of *Shigella* infection, the rectocolon. In this regard, expression of MAM on the surface of probiotic bacteria such as *Lactobacillus* might be more practical. *Shigella* infection elicits antibodies against invasion plasmid antigens (Ipa proteins) which does not offer protection. *Shigella* infection or vaccination also elicit serotype-specific antibodies that offer limited protection, which is not long lasting (Camacho *et al*., 2013). MAM is anticipated to induce a strong antibody response and again expression of MAM in probiotic bacteria may offer an alternative for protection against infection by all *Shigella* strains with functional MAM. Taken together, the present study has uncovered a novel adhesin contributing to *S. sonnei* pathogenesis. Because of its essential role during infection and its ability to trigger a strong immune response, *Shigella*MAM may offer future therapeutic potential in the prevention and treatment of shigellosis.

Experimental procedures

Bacterial strains and growth conditions

The bacterial wild-type strain used in this study was *Shigella sonnei* strain 20071599 (Xu *et al*., 2014) and mutants thereof. Bacteria were routinely grown on Congo red Trypticase soy agar (TSA) plates or in liquid LB at 37°C. For pMAM-His, 0.2 mM IPTG was added to the media to induce protein expression. To obtain EGFP expressing bacteria, strains

were transformed with pGEM-T-easy or pET28a containing EGFP. 100 μg ml^{-1} ampicillin or 50 μg ml^{-1}kanamycin was added for selection of plasmid containing strains. All primers and strains used in this study are listed in Tables S1 and S2.

Construction of *S. sonnei* deletion and complementation strains

Gene deletions in the *S. sonnei* 20071599 background (Xu *et al*., 2014) were constructed using the phage λ Red recombination system (Datsenko and Wanner, 2000). The plasmid, pKD46, which carries the red lambda recombinase genes, was transformed into strain 20071599. The kanamycin resistance cassette flanked by the first and last 51 base pairs of MAM coding sequences was amplified by PCR using primers a, b (Table S1) and used to replace the wild-type MAM gene via red lambda mediated homologs recombination (Fig. S1B). Plasmid, pCP20, was then introduced into the Kan-resistant mutant strain, allowing a second homologs recombination to loop out the Kan-cassette. The resultant strain, Δ*MAM*, harbored an in frame deletion with a scar of 102 base pairs (Fig. S1C). *icsA* and *MAM icsA* double knockout strains were constructed in the same way using primers g, h (Table S1). For complementation of the *MAM* deletion strain, the entire coding region of MAM SSO1327 was amplified with primers e and f (Table S1), which incorporated 6X histidine codons at the 3'-end of the MAM coding sequence. The PCR product was cloned into pGEM-T-Easy (ampR), with the 5'-end of the MAM coding sequence facing the *lacZ* promoter. The resultant clone was transformed into the Δ*MAM* mutant. For complementation of the *icsA* deletion strain, the promoter and entire coding sequence of SSOP143 *icsA/virG* gene was amplified with primers k and l (Table S1), which incorporated 5' EcoRl and 3' Sall restriction sites. The PCR product was cloned into pET28a (kanR). The resultant clone was transformed into the Δ*icsA* mutant. Plasmid, pMI, was constructed by cloning PCR-amplified *icsA* gene with its promoter using primers k_Pst and l_Pst. The PCR product was cut with PstI and cloned into the PstI-digested pMAM-6XHis clone. The resultant plasmid, pMI, was used to transform the *ΔMAMΔicsA*double mutant for complementation experiments. All steps of strain construction as well as complementation were confirmed by PCR and sequencing, using appropriate primers (Fig. S1C,D and Table S1).

Cell fractionation and Western blotting to determine MAM localization

For membrane preparation, bacterial cultures were grown overnight at 18°C, harvested by centrifugation (3500 rpm, 20 min, 4°C), washed once with PBS and resuspended in fresh lysis buffer TE (20 mM Tris, 10 mM EDTA, pH 8.0). Cells were sonicated for 12 cycles (30 s on, 30 s off). Samples were first centrifuged at 15,000 × *g* for 45 min at 4°C to separate the supernatant. The supernatant fraction was then ultracentrifuged (60,000 × *g*, 1 h at 4°C). The

pellets were subjected to phase separation to obtain the membrane fraction. Pellets were resuspended in 200 µl of 10 mM Tris-HCI, pH 7.4, 150 mM NaCl, and 1% Triton X-114 at 0°C. For membrane protein separation, a cushion (300 µl) of 10 mM Tris HCl, pH 7.4, 150 mM NaCl, 6% (w/v) sucrose, and 0.06% Triton X-114 was placed first in 1.5 ml microfuge tube and then the protein sample was then overlaid. The tube was incubated at 30°C for 3 min before centrifugation for 3 min at 300 × g. After centrifugation, the detergent phase was clearly separated at the bottom of the tube as an oily droplet, while the aqueous phase was on the top. The aqueous layer was removed and received 0.5% fresh Triton X-114, the surfactant dissolution happened at 0°C and then overlaid on the sucrose cushion used before, incubated at 30°C for 3 min before centrifugation (Bordier C 1981). Finally, the oily droplets of detergent that assumed to have the amphiphilic integral membrane protein were analyzed by SDS-PAGE and Western blot.

OmpA was detected using the polyclonal antibody orb6940 (anti-OmpA), followed by incubation with Alexa Fluor 680 $F(ab)_2$ fragment of goat anti-rabbit immunoglobulin G (IgG). MAM-His was detected using the 6X-His epitope Tag antibody (His-H8), followed by incubation with anti-mouse Alexa 680. Membranes were then viewed and imaged using a multi wavelength scanner at 700 nm.

Analysis of MAM localization by immunostaining

All strains Δ*dsbA*, Δ*MAM*, Δ*MAM*/p*MAM*-His, and Δ*dsbA*/p*dsbA*-His, were transformed with pET28a containing EGFP. Bacteria were grown in LB to mid-log phase, and collected by centrifugation and washed once with PBS. Bacterial suspensions were then spotted on glass slides, left to dry, fixed by 4% paraformaldehyde for 10 min and then washed with PBS. Slides were treated with or without 0.1% Triton-X100 in PBS, and then washed with PBS, and blocked for 30 min with 5% BSA in PBS. Primary staining was done on both sets using 6X-His epitope tag antibody (His-H8) (1:10 dilution in PBS) at RT for 30 min. Secondary staining was done using TRITC-conjugated goat anti-mouse antibody at RT for 30 min. Stained samples were analyzed by imaging on a Nikon Eclipse Ti fluorescence microscope (Nikon UK Ltd) and images were prepared using Image J (open source, http://imagej.nih.gov/ij/) and Corel Draw X5 (Nikon, Japan) (Corel Corporation, Ottawa, Canada).

Adherence and invasion assays on cultured cells

HEK293 and HeLa cells were routinely cultured at 37°C and under 5% CO_2 in Dulbecco's modified eagle medium (DMEM) containing 10% heat-inactivated fetal bovine serum, 110 mg L^{-1} sodium pyruvate, 10 ml L^{-1} of 100× non-essential amino acids, 100 units ml^{-1}penicillin and 20 µg ml^{-1} streptomycin. For adherence assays, bacteria were adjusted

to an MOI of 30 in DMEM without supplements and added to host cells. Plates were centrifuged (1000 × *g*, 22°C, 5 min) prior to incubation for 15 min at 37°C. Following infection, cells were washed thoroughly with PBS (at least three times), and lysed by addition of 0.1% Triton X-100 for 10 min. Lysates were serially diluted, plated on LB plates, incubated at 37°C overnight and colonies enumerated the next day. For PA depletion experiments, 50 μg ml^{-1}PLC was added to tissue culture cells for 15 min prior to infection, as previously described (Lim *et al*., 2014). Fibronectin-dependency was also tested as previously described (Krachler *et al*., 2012b), and bacterial cells were pre-incubated with fibronectin from human plasma (200 μg ml^{-1} in PBS) for 30 min prior to infection. For invasion assays, cells were infected with MOI of 10; bacteria were added to cells and centrifuged (2000 rpm, 22°C, 10 min), and incubated for 40 min. Following this, cells were washed with PBS prior to addition of 1 ml $well^{-1}$ of DMEM containing 50 μg ml^{-1} gentamycin. The plate was then incubated for a further 2 h, cells washed three times with PBS, lysed and colony forming units determined using dilution plating, as described earlier. When testing the effect of MAM beads on invasion, host cells were treated with 5 μM MAM beads or control (GST-coupled) beads for 30 min prior to invasion assays. Technical details of bead synthesis and molar ratio calculation have been described previously (Krachler and Orth, 2013, Stones *et al*., 2015).

Analysis of TTSS effector production and secretion by Western blotting

Colonies were picked from Congo red plates, and bacteria were grown in TSB to mid-log phase. Cells were pelleted, washed with sterile PBS, resuspended in fresh PBS containing 0.01% Congo red and incubated at 37°C for 30 min. When MAM and control beads were tested for their ability to interfere with TTSS, they were added at a final concentration of 10 μM prior to the 30 min incubation. Cells were then centrifuged to separate samples into pellet fraction (to give total lysates reflecting protein production) and supernatants (to check for protein secretion). Pellets were washed once with PBS and boiled in sample buffer. Supernatants were used to precipitate proteins by precipitation with 10% TCA, as described previously (Yu *et al*., 2000). Following TCA addition, samples were incubated on ice for 20 min prior to centrifugation to pellet proteins (14,000 rpm, 4°C, 20 min). Protein pellets were washed in 70% ethanol, dried, resuspended in SDS-PAGE sample buffer and boiled for 5 min. Samples were separated by SDS-PAGE and IpaB and IpaC were detected by Western blotting using the monoclonal antibodies H16 (anti-IpaB) and J22 (anti-IpaC), respectively (Yu *et al*., 2000) followed by Alexa Fluor 680 goat anti-mouse IgG and membranes were imaged on a multi wavelength scanner at 700 nm.

Analysis of TTSS effector translocation by Förster resonance energy transfer

In order to use red lambda system to create an *ipgD*-TEM fusion (*ipgD* encodes a TTSS substrate and TEM encode β-lactamase), we modified Plasmid pkD46 for kanamycin resistance instead of ampicillin resistance. By using inverse PCR the whole pkD46 except *bla*was amplified using primers w and x (Table S1). The purified inverse PCR product as well as Kan-cassette PCR product using pkD4 plasmid as template with primers u and v (Table S1), were digested using BglII restriction enzyme, then ligated and electroporated into DH5α. Colonies were selected on Kan/LB agar and the pKD46/pKD4 plasmid was extracted and verified for the right direction using XhoI and HindIII enzymes. The new pKD46/pKD4 plasmid was introduced into both wild type and Δ*MAM*. The TEM gene was introduced to these two strains using primers s and t (Table S1), which resulted in an *ipgD*-TEM in frame fusion. The empty pGEM-T-Easy (ampR) plasmid was transformed into wild type and *ΔMAM* to serve as negative controls. The constructed strains both possessed β-lactamase activity and compared with negative controls (wild-type strain), by use of nitrocefin discs according to the manufacturer's protocol (Oxoid, Hampshire, UK). Briefly, pure colonies of all strains were picked, suspended in PBS and applied directly to the discs and discs were incubated at 22°C for 30 min. Positive reaction was identified by red colored discs (Fig. S2). For FRET assays, 6X CCF4-AM substrate loading solution was prepared, 10^6 cells of HEK293 cells were prepared in 100 µl of EM buffer (120 mM NaCl, 7 mM KCl, 1.8 mM $CaCl_2$, 0.8 mM $MgCl_2$, 5 mM glucose) (Nothelfer *et al*., 2011). 20 µl of 6X CCF4-AM were added to each tube of 100 µl of the cells and incubated in the dark at 22°C for 1 h. Fluorescence Resonance Energy Transfer (FRET) reporter strains were added to HEK293 cells at an MOI of 100 in DMEM and centrifuged (300 g, 10 min, 22°C) prior to incubation at 37°C for 50 min (Nothelfer *et al*., 2011). Cells were washed once with PBS, and the infection was stopped by adding EM buffer containing 50 µg ml^{-1} gentamycin. Cells were fixed with 4% paraformaldehyde and mounted on glass slides for FRET imaging, using a Nikon A1R confocal fluorescence microscope. Ratiometric analysis was done using Image J. Alternatively; cells were subjected to analysis by flow cytometry (excitation 355 nm, and emission 457 nm for coumarin and emission 529 nm for fluorescein).

G. mellonella larvae infection model

Bacterial strains were grown to mid-log phase in LB to prepare stocks for infections. For each experimental condition, 10 healthy 2- to 3-day-old larvae of approximately equal weight were infected with *S. sonnei* strains by injection of 10 µl total volume into the front, right proleg. The control group received the same volume of sterile PBS buffer instead. Two infectious doses (10^5 CFU and 10^6 CFU) were tested. As a dose of 10^6 CFU *S. sonnei* wild-type strain

caused mortality within one day, the lower dose was used for subsequent experiments; exceptions are stated in the figure legend. For MAM bead protection experiments, larvae were co-injected with 10 µl total volume containing a mixture of either 10^5 CFU or 10^6 CFU *S. sonnei* wild-type bacteria and 6–25 µM MAM or GST (control) beads. Preparation of MAM beads has been described elsewhere (Lim *et al*., 2014). To study the effects of DOC treatment on infection, larvae were challenged with *S. sonnei* strains grown overnight with or without DOC (2.5 mM). Following infection, larvae were incubated at 37°C and larval survival was scored daily, for five days. Larvae were scored as dead when they no longer responded to touch. Survival data were analyzed using the Kaplan–Meier estimator. Survival curves were compared using the Mantel–Cox log–rank test and differences in the mortality of larvae infected with wild-type and Δ*MAM* strains were significantly different ($P < 0.0001$).

G. mellonella hemolymph processing for flow cytometry and microscopy

Following 4 h of infection, hemolymph of 10 larvae per experimental condition was collected by making an incision between the two segments nearest the larvae tail to avoid gut disruption. Hemolymph was collected in 0.5 ml of sterile PBS and processed within 10 min to prevent clotting (Harding *et al*., 2013). For imaging, hemolymph was transferred to a glass coverslip in a 24-well plate; 0.5 ml of PBS was added and mixed well. The plate was then centrifuged at 2000 rpm for 10 min at room temperature using an aerosol-tight centrifuge plate holder. The supernatant was carefully removed and cells were washed with PBS. Cells were fixed in 4% (v/v) paraformaldehyde in PBS for 10 min. 0.5 ml of 15 mM NH_4Cl in PBS was used to quench residual paraformaldehyde and the plate was incubated at RT for 15 min. Afterwards, cells were permeabilized for 5 min at RT using 0.5 ml of 0.1% Triton X-100 in PBS. Blocking was done for 1 h using 2% (w/v) BSA in PBS, and then cells were stained with Alexa Flour 548-phalloidin and Hoechst. Samples were mounted and cured overnight prior to imaging. For flow cytometry, hemolymph was centrifuged at 2000 rpm for 10 min at RT, and hemocytes were resuspended in 1 ml PBS containing 4% (v/v) paraformaldehyde in PBS for fixation. Cells were vigorously mixed and then were used for flow cytometry. For analysis, lasers emitting at 488 nm were used for detection of EGFP expressing bacteria. Data acquisition and analysis was performed using Kaluza™ software (Beckman Coulter, Brea, USA).

qPCR analysis of icsA and MAM transcription

Wild-type *S. sonnei* strain was grown in the presence or absence of 2.5 mM DOC overnight in L-broth with shaking (200 rpm). RNA was isolated using a Total RNA kit (Bioline). The house-keeping gene, *cycG*, was used as an internal control. Primers y,z; y1,z1 and y2,z2

(Table S1) were used to prepare cDNA for *icsA, MAM* and *cycG* genes, respectively. To establish standard curves for each gene, a serial dilution (from 100 to 10^8 molecules μl^{-1}) of bacterial genomic DNA was used for PCR using SYBR-Green QRT-PCR kit on Rotor Gene 6000 (Qiagen, Life Sciences and Technology UK). Changes in gene expression between untreated and DOC-treated cultures were calculated using the $2^{-\Delta\Delta ct}$ method and proprietary software in the Rotor Gene instrument (version 1.7.34). Triplicate RNA samples from triplicate cultures ($n = 3$) were used to prepare cDNAs, which were quantified by the same PCR procedure. The amplification curves of *MAM* and *icsA* were normalized with that of *cycG*, and quantification was calculated using the standard curves. The levels of transcripts from bacteria grown in the absence of DOC were set as calibrator and levels of transcripts from bacteria grown in the presence of DOC were expressed as $\log 2^{-\Delta\Delta ct}$.

Guinea pig keratoconjunctivitis model (Sereny test)

Experimental protocols involving guinea pigs were performed with approval of Xi'an Jiao Tong University ethics committee. Guinea pigs 6–8 weeks old, weighing 200–300 g, were infected with 5×10^8 CFU per eye of *S. sonnei* wild-type or Δ*MAM* strains, as previously described (Xu *et al*., 2014). For testing DOC regulation, wild-type *S. sonnei* was grown overnight in the presence or absence of 2.5 mM DOC. Development of keratoconjunctivitis was monitored and scored daily up to 14 days.

Immunization experiments

Guinea pigs ($n = 3$) were infected with 5×10^8 of Δ*MAM* strain per eye at days 1, 14 and 28. On day 31, wild-type *S. sonnei* (5×10^8 CFU per eye) were used to challenge the animals. Animals were observed daily for development of keratocunjunctivitis. A second group of guinea pigs ($n = 3$) were immunized with Δ*MAM* strain on days 1, 14, 28, 32 and 48. On day 51, animals of the immunization group as well as those challenged with wild-type *S. sonnei* were sacrificed. Spleen lymphocytes were isolated for detecting specific ASCs against *S. sonnei* by ELISPOT. All procedures were described previously (Xu *et al*., 2014).

Ethics statement

The animal experiments in this study were approved by the Laboratory Animal Administration Committee of Xi'an Jiaotong University under the licence (No XJTU2014-102), and performed according to the guidelines of Animal Experimentation of Xi'an Jiaotong University, The Guideline on the Care and Use of Laboratory Animals issued by the Chinese Council on Animal Research, and The Guide for the Care and Use of Laboratory Animal published by the US National Institute of Health (NIH publication No. 85-23, revised 2011).

We carry out our best laboratory practice to ensure animals suffer from minimal stress during all experiments.

Acknowledgements

The authors would like to thank members of the Krachler and Yu labs for critical reading and useful comments on the manuscript. We also thank Jian Yang for Bioinformatics and Stuart Wood and Clare Harding for technical assistance. This work was supported by grants from the BBSRC (DHS and AMK). Rasha Y. Mahmoud is supported by the The Channel Scheme of the Egyptian Culture Council.

Author contributions

Conceived and designed experiments: AMK and JY. Performed the experiments: RYM, DHS, WL, DW and YW. Analyzed the data: RYM, DHS, AMK and JY. Contributed reagents/materials/analysis tools: DHS, AMK, JY, ME and ERA. Wrote the article: RYM, AMK and JY.

Conflict of interest

The authors declare no conflicts of interest.

References

Bahrani, F.K., Sansonetti, P.J., and Parsot, C. (1997) Secretion of Ipa proteins by *Shigella flexneri*: inducer molecules and kinetics of activation. *Infect Immun* **65**: 4005–4010.

Bernardini, M.L., Mounier, J., d'Hauteville, H., Coquis-Rondon, M., and Sansonetti, P.J. (1989) Identification of icsA, a plasmid locus of *Shigella flexneri* that governs bacterial intra- and intercellular spread through interaction with F-actin. *Proc Natl Acad Sci USA* **86**: 3867–3871.

Bordier, C. (1981) Phase separation of integral membrane proteins in Triton X-114 solution. *J Biol Chem* **256**: 1604–1607.

Brotcke Zumsteg, A., Goosmann, C., Brinkmann, V., Morona, R., and Zychlinsky, A. (2014) IcsA is a *Shigella flexneri* adhesin regulated by the type III secretion system and required for pathogenesis. *Cell Host Microbe* **15**: 435–445.

Camacho, A.I., Irache, J.M., and Gamazo, C. (2013) Recent progress towards development of a *Shigella* vaccine. *Expert Rev Vaccines* **12**: 43–55.

Chen, K.T., Chen, C.J., and Chiu, J.P. (2001) A school waterborne outbreak involving both *Shigella sonnei* and *Entamoeba histolytica*. *J Environ Health* **64**: 9–13, 26.

Chen, Y., Smith, M.R., Thirumalai, K., and Zychlinsky, A. (1996) A bacterial invasin induces macrophage apoptosis by binding directly to ICE. *EMBO J* **15**: 3853–3860.

Datsenko, K.A., and Wanner, B.L. (2000) One-step inactivation of chromosomal genes in *Escherichia coli* K-12 using PCR products. *Proc Natl Acad Sci USA* **97**: 6640–6645.

DuPont, H.L., Levine, M.M., Hornick, R.B., and Formal, S.B. (1989) Inoculum size in shigellosis and implications for expected mode of transmission. *J Infect Dis* **159**: 1126–1128.

Eitel, J., and Dersch, P. (2002) The YadA protein of *Yersinia pseudotuberculosis* mediates high-efficiency uptake into human cells under environmental conditions in which invasin is repressed Infect. *Immun* 704880–704891.

Harding, C.R., Schroeder, G.N., Reynolds, S., Kosta, A., Collins, J.W., Mousnier, A., and Frankel, G. (2012) *Legionella pneumophila* pathogenesis in the *Galleria mellonella* infection model. *Infect Immun***80**: 2780–2790.

Harding, C.R., Schroeder, G.N., Collins, J.W., and Frankel, G. (2013) Use of *Galleria mellonella* as a model organism to study *Legionella pneumophila* infection. *J Visual Exp* **81**: e50964.

Hawley, C.A., Watson, C.A., Orth, K., and Krachler, A.M. (2013) A MAM7 peptide-based inhibitor of *Staphylococcus aureus* adhesion does not interfere with *in vitro* host cell function. *PLoS ONE* **8**: e81216.

High, N., Mounier, J., Prevost, M.C., and Sansonetti, P.J. (1992) IpaB of *Shigella flexneri* causes entry into epithelial cells and escape from the phagocytic vacuole. *EMBO J* **11**: 1991–1999.

Holt, K.E., Baker, S., Weill, F.X., Holmes, E.C., Kitchen, A., Yu, J., *et al*. (2012) *Shigella sonnei* genome sequencing and phylogenetic analysis indicate recent global dissemination from Europe. *Nat Genet***44**: 1056–1059.

Islam, D., Ruamsap, N., Khantapura, P., Aksomboon, A., Srijan, A., Wongstitwilairoong, B., *et al*. (2014) Evaluation of an intragastric challenge model for *Shigella dysenteriae* 1 in rhesus monkeys (*Macaca mulatta*) for the pre-clinical assessment of *Shigella* vaccine formulations. *APMIS* **122**: 463–475.

Jaglic, Z., Desvaux, M., Weiss, A., Nesse, L.L., Meyer, R.L., Demnerova, K., *et al*. (2014) Surface adhesins and exopolymers of selected foodborne pathogens. *Microbiology* **160**: 2561–2582.

Khoa, D.B., Trang, L.T., and Takeda, M. (2012) Expression analyses of caspase-1 and related activities in the midgut of *Galleria mellonella* during metamorphosis. *Insect Mol Biol* **21**: 247–256.

Kotloff, K.L., Winickoff, J.P., Ivanoff, B., Clemens, J.D., Swerdlow, D.L., Sansonetti, P.J., *et al*. (1999) Global burden of *Shigella* infections: implications for vaccine development and implementation of control strategies. *Bull World Health Organ* **77**: 651–666.

Krachler, A.M., and Orth, K. (2011) Functional characterization of the interaction between bacterial adhesin multivalent adhesion molecule 7 (MAM7) protein and its host cell ligands. *J Biol Chem* **286**: 38939–38947.

Krachler, A.M., and Orth, K. (2013) Targeting the bacteria–host interface: strategies in anti-adhesion therapy. *Virulence* **4**: 284–294.

Krachler, A.M., Ham, H., and Orth, K. (2011) Outer membrane adhesion factor multivalent adhesion molecule 7 initiates host cell binding during infection by gram-negative pathogens. *Proc Natl Acad Sci USA* **108**: 11614–11619.

Krachler, A.M., Ham, H., and Orth, K. (2012a) Turnabout is fair play: use of the bacterial multivalent adhesion molecule 7 as an antimicrobial agent. *Virulence* **3**: 68–71.

Krachler, A.M., Mende, K., Murray, C., and Orth, K. (2012b) *In vitro* characterization of multivalent adhesion molecule 7-based inhibition of multidrug-resistant bacteria isolated from wounded military personnel. *Virulence* **3**: 389–399.

Leclerc, H., Schwartzbrod, L., and Dei-Cas, E. (2002) Microbial agents associated with waterborne diseases. *Crit Rev Microbiol* **28**: 371–409.

Leuko, S., and Raivio, T.L. (2012) Mutations that impact the enteropathogenic *Escherichia coli* Cpx envelope stress response attenuate virulence in *Galleria mellonella*. *Infect Immun* **80**: 3077–3085.

Lim, J., Stones, D.H., Hawley, C.A., Watson, C.A., and Krachler, A.M. (2014) Multivalent adhesion molecule 7 clusters act as signaling platform for host cellular GTPase activation and facilitate epithelial barrier dysfunction. *PLoS Pathog* **10**: e1004421.

Menard, R., Sansonetti, P., and Parsot, C. (1994) The secretion of the *Shigella flexneri* Ipa invasins is activated by epithelial cells and controlled by IpaB and IpaD. *EMBO J* **13**: 5293–5302.

Mounier, J., Bahrani, F.K., and Sansonetti, P.J. (1997) Secretion of *Shigella flexneri* Ipa invasins on contact with epithelial cells and subsequent entry of the bacterium into cells are growth stage dependent. *Infect Immun* **65**: 774–782.

Niebuhr, K., Jouihri, N., Allaoui, A., Gounon, P., Sansonetti, P.J., and Parsot, C. (2000) IpgD, a protein secreted by the type III secretion machinery of *Shigella flexneri*, is chaperoned by IpgE and implicated in entry focus formation. *Mol Microbiol* **38**: 8–19.

Niyogi, S.K. (2005) Shigellosis. *J Microbiol* **43**: 133–143.

Nothelfer, K., Dias Rodrigues, C., Bobard, A., Phalipon, A., and Enninga, J. (2011) Monitoring *Shigella flexneri* vacuolar escape by flow cytometry. *Virulence* **2**: 54–57.

Page, A.L., Ohayon, H., Sansonetti, P.J., and Parsot, C. (1999) The secreted IpaB and IpaC invasins and their cytoplasmic chaperone IpgC are required for intercellular dissemination of *Shigella flexneri*. *Cell Microbiol* **1**: 183–193.

Philpott, D.J., Edgeworth, J.D., and Sansonetti, P.J. (2000) The pathogenesis of *Shigella flexneri*infection: lessons from *in vitro* and *in vivo* studies. *Philos Trans R Soc Lond B Biol Sci* **355**: 575–586.

Rahman, K.M., Arifeen, S.E., Zaman, K., Rahman, M., Raqib, R., Yunus, M., *et al*. (2011) Safety, dose, immunogenicity, and transmissibility of an oral live attenuated *Shigella flexneri* 2a vaccine candidate (SC602) among healthy adults and school children in Matlab, Bangladesh. *Vaccine* **29**: 1347–1354.

Ranjbar, R., Aleo, A., Giammanco, G.M., Dionisi, A.M., Sadeghifard, N., and Mammina, C. (2007) Genetic relatedness among isolates of *Shigella sonnei* carrying class 2 integrons in Tehran, Iran, 2002–2003. *BMC Infect Dis* **7**: 62.

Rosqvist, R., Forsberg, A., Rimpilainen, M., Bergman, T., and Wolf-Watz, H. (1990) The cytotoxic protein YopE of *Yersinia* obstructs the primary host defence. *Mol Microbiol* **4**: 657–667.

Schroeder, G.N., and Hilbi, H. (2008) Molecular patjhogenesis of *Shigella* spp.: controlling host signaling, invasion, and death by type III secretion. *Clin Microbiol Rev* **21**: 134–156.

Seol, S.Y., Kim, Y.T., Jeong, Y.S., Oh, J.Y., Kang, H.Y., Moon, D.C., *et al*. (2006) Molecular characterization of antimicrobial resistance in *Shigella sonnei* isolates in Korea. *J Med Microbiol* **55**: 871–877.

Stones, D.H., Al-Saedi, F., Vaz, D., Perez-Soto, N., and Krachler, A.M. (2015) Biomimetic materials to characterize bacteria-host interactions. *J Vis Exp.* In press (e53400, doi:10.3791/53400).

Thirumalai, K., Kim, K.S., and Zychlinsky, A. (1997) IpaB, a *Shigella flexneri* invasin, colocalizes with interleukin-1 beta-converting enzyme in the cytoplasm of macrophages. *Infect Immun* **65**: 787–793.

Veenendaal, A.K., Hodgkinson, J.L., Schwarzer, L., Stabat, D., Zenk, S.F., and Blocker, A.J. (2007) The type III secretion system needle tip complex mediates host cell sensing and translocon insertion. *Mol Microbiol* **63**: 1719–1730.

Viegas, S.C., Mil-Homens, D., Fialho, A.M., and Arraiano, C.M. (2013) The virulence of *Salmonella enterica* Serovar Typhimurium in the insect model *Galleria mellonella* is impaired by mutations in RNase E and RNase III. *Appl Environ Microbiol* **79**: 6124–6133.

WHO (2006) Future needs and directions for *Shigella* vaccines. *Wkly Epidemiol Rec* **81**: 51–58.

Xu, D., Yang, X., Wang, D., Yu, J., and Wang, Y. (2014) Surface display of the HPV L1 capsid protein by the autotransporter *Shigella* IcsA. *J Microbiol* **52**: 77–82.

Yang, F., Yang, J., Zhang, X., Chen, L., Jiang, Y., Yan, Y., *et al*. (2005) Genome dynamics and diversity of *Shigella* species, the etiologic agents of bacillary dysentery. *Nucleic Acids Res* **33**: 6445–6458.

Yu, J., Edwards-Jones, B., Neyrolles, O., and Kroll, J.S. (2000) Key role for DsbA in cell-to-cell spread of *Shigella* flexneri, permitting secretion of Ipa proteins into interepithelial protrusions. *Infect Immun* **68**: 6449–6456.

Zychlinsky, A., Prevost, M.C., and Sansonetti, P.J. (1992) *Shigella flexneri* induces apoptosis in infected macrophages. *Nature* **358**: 167–169.